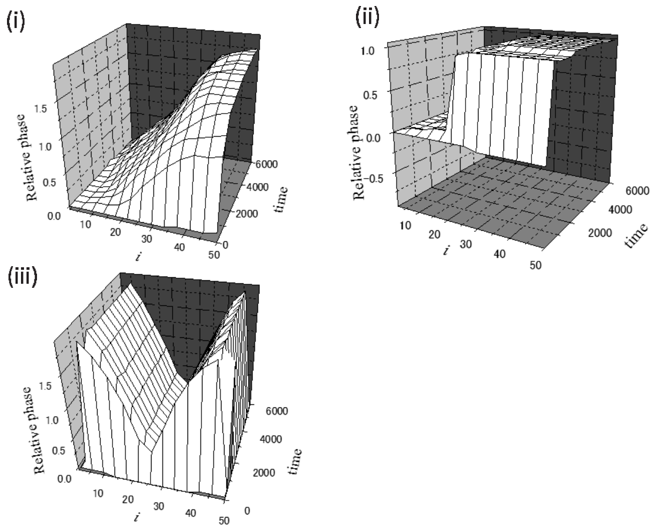

Fig. 7. Temporal evolutions of the relative phases ψ_i obtained from the simulation of Eq. (14) when the target state is (i) unidirectional phase-shifted state, (ii) 2-cluster state, and (iii) "v-type" phase-shifted state. The initial condition is set at $u_i = v_i = 1.5$ for all i. The definition of the relative phase ψ_i is described in the text. Since the relative phase is 2π-periodic, it is expressed within the range of (i)(iii) $[-0.05\pi, 1.95\pi]$ and (ii) $[-0.95\pi, 1.05\pi]$.

of the harmonics in which $q_f(\psi)$ has nonnegligible Fourier components.

The functional form of the target coupling function $\tilde{q}(\psi)$, the positions of the nodes s_γ and s_β, and the parameter $\epsilon'_{\beta\gamma}$ are selected such that the target state is obtained. They are explored through the simulation of Eq. (8) by trial and error, with taking notice that $\mathrm{Max}[|A_k|, |B_k|]$ does not have a large value. Figure 3 shows the temporal evolutions of the phase difference between the first and ith oscillators obtained from the simulation of Eq. (8) with the initial condition of $\phi_i = 0$ for all i when $\tilde{q}(\psi)$ and the positions of the nodes are given as shown in Figs. 4 and 5, respectively. Here, $\epsilon'_{\beta\gamma}$ is set at 0.05 when the measurement and stimulation nodes in Fig. 5 are connected by an arrow, otherwise $\epsilon'_{\beta\gamma} = 0$. It is found that the target states described above are actually obtained under these conditions. $\epsilon'_{\beta\gamma}$, because changing only $\tilde{q}(\psi)$ is often insufficient to obtain the target state.

Next, the parameters τ_m and Γ_m are determined using the obtained coupling functions $q_f(\psi)$ and $\tilde{q}(\psi)$. Figure 6 shows the relation between α and $\sum_{m=1}^{2M+1} |\Gamma_m|$ obtained from Eqs. (12) and (13) in the case of $\tilde{q}(\psi) = \sin\psi + 0.5\sin2\psi + 0.5\cos\psi$ (Fig. 4(iii)). It is found that $\sum_{m=1}^{2M+1} |\Gamma_m|$ varies significantly with α. Since we need to select the parameter sets of τ_m and Γ_m such that $\sum_{m=1}^{2M+1} |\Gamma_m|$ can be possibly minimized, we have selected them using the value of α where $\sum_{m=1}^{2M+1} |\Gamma_m|$ becomes minimum.

Then, Eq. (14) is simulated using the obtained values of τ_m and Γ_m. Figure 7 shows the temporal evolutions of the relative phases of the oscillators. Here, the relative phase of the ith oscillator ψ_i ($i = 2, 3, \ldots$, and 50) is defined as $\psi_i(t_1^{(K)}) = 2\pi(t_1^{(K+1)} - t_i^{(K')})/(t_1^{(K+1)} - t_1^{(K)}) + 2\pi n$, where n is an arbitrary integer, and $t_1^{(K)}$ and $t_i^{(K')}$ denote the time when the first and ith oscillators take maximum values of u at the Kth and K'th cycles, respectively, with K and K' satisfying $t_1^{(K)} \leq t_i^{(K')} < t_1^{(K+1)}$. It is found that the states obtained through the feedback are generally in good agreement with those obtained from the simulation of Eq. (8) (Fig. 3), although not completely. Thus, the dynamical behaviors are well controlled by the feedback.

4. Discussion

We have proposed a generalized method to control the dynamics of coupled oscillators by designing the coupling function through multi-linear feedback, and have confirmed its validity through a simulation of one-dimensionally-arranged Bonhoeffer-van der Pol oscillators. Our previous theory (Kano and Kinoshita, 2008) is only applicable to a special case where the oscillators are coupled to each other by the same coupling strength and the observable is measured uniformly from all of the oscillators with the feedback signals uniformly applied to all of them. In contrast, the present theory is even applicable to systems where the coupling strengths, the observables, and the applied feedback signals are not uniform. Such generalization is extremely important, because they are not uniform in most of actual coupled-oscillator systems. Hence, it is expected that the present method will lead to various practical applications.

The most characteristic point of the present method is that it requires only the outputs from several measurement nodes to determine the delays and the strengths of feedback signals, whereas the method reported by Kiss *et al.* (2007) and Kori *et al.* (2008) required an individual output from each oscillator. This is extremely advantageous because it is often practically difficult to measure individual outputs from all oscillators and to process them rapidly, particularly when the number of oscillators becomes large. Thus, the present method will eventually be used without practical restrictions.

When $\mathrm{Max}[|A_k|, |B_k|]$ is large, the present method is not applicable because $\sum_{m=1}^{2M+1} |\Gamma_m|$ becomes large. Hence, $\tilde{q}(\psi)$ cannot have large Fourier components in the harmonics where $q_f(\psi)$ has small components. In spite of such restriction, in most of cases we can select $\tilde{q}(\psi)$ that leads